

# Type of materials, pyrolysis conditions, carbon content and size dimensions: the parameters that influence the mechanical properties of biochar cement-based composites

Isabella Cosentino<sup>a</sup>, Luciana Restuccia<sup>a</sup>, Giuseppe Andrea Ferro<sup>a</sup>, Jean-Marc Tulliani<sup>b</sup>

<sup>a</sup>*Department of Structural, Geotechnical and Building Engineering, Politecnico di Torino, 10129 Turin (Italy)*

<sup>b</sup>*Department of Applied Science and Technology, Politecnico di Torino, 10129 Turin (Italy)*

1 **ABSTRACT:** Interest in biochar, a sub-product of biomass pyrolysis, has increased enormously in the last  
2 few years, finding applications in a wide variety of fields. In the present work, a standardized biochar was used  
3 as a nano filler in cement-based composites, ensuring the reproducibility of cement mixtures.  
4 Although, in terms of flexural strength and fracture energy, results were inferior compared to the previous  
5 studies conducted at Politecnico di Torino. Nonetheless, an overall enhancement of mechanical properties was  
6 recorded with the introduction of standardized biochar in cementitious composites. This paper attempts to  
7 show that some parameters of biochar processes, e.g. production, temperature, heating rate or pressure, as well  
8 as some biochar features such as carbon content, particle size distribution or porosity dramatically influence  
9 the enhancement of mechanical properties of cementitious composites. This result is extremely important,  
10 because it indicates that, even if the parameters are not optimal, biochar can be used to create new green  
11 building materials because of its effectiveness in cementitious composites.

12

13 **Key words:** pyrolysis; biochar; cement-based composites; carbon nanoparticles; mechanical properties;  
14 fracture energy.

15

16

## 17 **1. Introduction**

18 The cement industry is currently facing multiple challenges such as: depletion of fossil fuel reserves, scarcity  
19 of raw materials, increasing demand for construction materials, as well as increasing environmental concerns

20 such as air pollution and climate change. The production of Ordinary Portland Cement (OPC) yearly releases  
21 into the atmosphere roughly 6% of all man-made carbon dioxide emissions [1]. This makes cement the most  
22 studied material and the use of green concrete is spreading through partial substitution of raw materials and  
23 partial replacement of clinker with alternative constituents such as fly ashes, blast-furnace slag, silica fume  
24 (Supplementary Cementitious Materials, SCMs) or leading to the development of alternative binders such as  
25 calcium sulfoaluminate cement, magnesium oxide based cement, geopolymers, CO<sub>2</sub>-cured cement (Alternative  
26 Cementitious Materials, ACMs).

27 An emerging material called biochar is receiving increasing attention, given its extraordinary chemical and  
28 physical properties and above all because it is a waste product which is difficult to dispose of. In fact, it derives  
29 from the pyrolysis process, which is the thermal decomposition of biomass in a limited or zero oxygen  
30 environment [2]. Biochar is a fine, porous and light material, with a great absorption capacity and a large  
31 surface area. Furthermore, it has a basic pH and is rich in carbon. Biochar is chemically stable for long periods  
32 of time (hundreds or thousands of years) and, consequently, it is believed that it could be effective for long-  
33 term CO<sub>2</sub> sequestration [3-4]. Biochar is used mainly in agriculture as a soil improver, that increases soil  
34 fertility and allows the capture of carbon in soils, thus contributing to the mitigation of climate change [5]. It  
35 is used as a food supplement in cattle breeding, as a reducing agent for metal production in industrial processing  
36 and to clean grey water. Another field is the textile industry: here it is introduced as a component of fabrics for  
37 sportswear and can perform the functions of an absorber. It is also experimented inside batteries, because of  
38 its propensity to be a chemical reducing agent. It also finds application as a component in asphalts. Moreover,  
39 biochar has excellent insulating properties and it can also act as a filter for the air because of its porous  
40 structure, improving air quality. It can therefore easily absorb moisture and work as humidity sensors, as well  
41 [6,7] as electromagnetic shielding [8]. Furthermore, it can be used as an insulating material in buildings [9].  
42 Biochar has been investigated at Politecnico di Torino for several years as nano/micro particles in cement-  
43 based composites, in order to obtain an enhancement of mechanical properties of cementitious materials [10].  
44 It has been proved that biochar can be easily inserted into the cement mixture as a filler, since it does not react  
45 with the cement matrix, and at nano/micro scale it reduces the porosity and consequently improves the  
46 durability of concrete. Politecnico di Torino research has focused attention on agro-food industry waste: coffee

47 powder, cocoa husks, pellets of parchment coffee, rice husk and hazelnut shells and many others. This waste  
48 has been pyrolyzed via a lab-scale reactor system, evaluating its contribution to cementitious composites.  
49 Results of this research are summarized here.

50 1. Micro-carbonized particles obtained from hemp hurd (HH) by controlled pyrolysis were used as the  
51 additive in self-consolidating cement composites. In [10], an investigation on four different additions  
52 (i.e. 0.08, 0.20, 1.00 and 3.00 by wt% of biochar in cement) is reported. The analysis of flexural  
53 strength values showed a mixed trend of increase and decrease in proportion to variations of the  
54 content of carbonized particles addition. A slight increase of 7% in the modulus of rupture, MOR, was  
55 achieved by adding 0.08 wt% HH, while a noticeable decrease occurred on further additions up to 3%.  
56 Evaluated toughness indices of cement composites (I5 & I10, determined according to the standard  
57 ASTM C1018 [11]) clearly demonstrated that the addition of HH significantly increased the fracture  
58 toughness. It is believed that the presence of a high number of irregular-shaped carbonized particles  
59 influences the crack paths by increasing their tortuosity [10].

60 2. Pyrolyzed polyethylene beads (CNBs) and coconuts shells (*Cocos nucifera*, CCNs) were produced to  
61 investigate the potential beneficial effects of carbon micro/nanoparticle addition to cement pastes to  
62 improve mechanical properties of the resulting composites. When up to 0.08 wt% was added to cement  
63 paste, both pyrolyzed CNBs and CCNs proved to be effective in increasing the cement matrix  
64 compressive strength and toughness. Aggregate shape is critical for toughening and angular grains are  
65 needed to produce effective aggregate-bridging. Carbon nano/micro-particles were prepared by  
66 chemical vapor deposition (CVD) using low-density polyethylene (LDPE) as a precursor. These  
67 particles proved to be spherical and interconnected for the CNBs, while the CCNs were irregular in  
68 shape, as a result of the grinding step. A pressure of 3 bars was fixed inside the reacting chamber while  
69 the temperature was maintained in the range 750-850°C and an inert carrier gas was used in the  
70 experiment [12].

71 3. Nano/micro carbonized particles produced from waste bagasse fibers were explored to modify  
72 mechanical properties and fracture patterns of the resulting cementitious composites. When added to  
73 cement paste up to 1 wt% (six different amounts were investigated), the carbonized bagasse particles

74 were found to be significant in improving mechanical strength as well as fracture toughness. The  
75 increment of mechanical strength was observed up to an addition of 0.2 wt%. Also in this case, an  
76 inverse trend was observed beyond this quantity. Results demonstrated that an addition of these  
77 carbonized particles by 0.2wt% improved the flexural resistance measured in terms of MOR by 69.9%  
78 while an increment of 46.4% and 61.2% was achieved in first crack and ultimate fracture toughness,  
79 respectively. The importance of the particle shape on toughening is therefore critical and angular grains  
80 are needed to produce effective crack-bridging [13].

81 4. Nano/micro-sized carbonized particles were synthesized from hazelnut and peanut shells to produce  
82 high-performance cement composites. Carbon nano/microparticles obtained by controlled pyrolysis  
83 of peanut (PS) and hazelnut (HS) shells were investigated. When added to cement paste, up to 1 wt%,  
84 these materials led to an increase in the cement matrix flexural strength and toughness. Moreover, with  
85 respect to plain cement, the total increase in electromagnetic radiation shielding effect obtained by  
86 adding 0.5 wt% of PS or HS in cement composites was much higher in comparison to the ones reported  
87 in the literature for CNTs used in the same quantity. In the case of PS addition, the percentage of  
88 particles which ensured maximum shielding effectiveness also coincided with maximum value of  
89 fracture energy, making it possible to prepare cementitious materials optimized both from a  
90 mechanical and an electromagnetic shielding point of view [8].

91 5. Cement composites are quasi-brittle in nature and possess extremely low tensile strength compared to  
92 their compressive strength. Experimental results indicated that the incorporation of micro sized inert  
93 particles acted as obstacles in the growth of the cracks, thus improving the ductility and the energy  
94 absorption capacity of the self-consolidating cementitious composites [14].

95 6. Nano/micro-sized pyrolyzed hazelnut shells and pyrolyzed coffee powder particles were used as “zero  
96 cost” aggregates in cement pastes, in order to improve strength and toughness. Results showed an  
97 increase of mechanical properties of tested specimens, specifically an improvement in strength,  
98 toughness and ductility. Furthermore, mechanical properties strongly improved for certain specific  
99 quantities of carbonized nano-micro materials (0.8 wt% with respect to cement). Pyrolyzed nano/micro  
100 particles can interact with the fracture evolution by means of the “overlapping effect”. Moreover, they

101 are strong enough to force a change of the path and the growth of microcracks, thus increasing the  
102 fracture surface and consequently fracture energy [15].

103 7. Two types of pyrolyzed agro-food waste, coffee powder and hazelnut shells, were investigated as  
104 carbon nano-aggregates, in different percentages of addition with respect to the cement weight. Results  
105 after 7 days curing showed that nanoparticles substantially improved all evaluated mechanical  
106 parameters with respect to the original cement-based composites. It can be notice that the two types of  
107 biochar “worked better” at different quantities. Analysis of the MOR results showed the most effective  
108 addition for pyrolyzed hazelnut shells was 0.8 wt%, while for coffee powder it was 0.5 wt%. Regarding  
109 the fracture energy results, the trend was similar to results for three-point bending, TPB, tests. Also  
110 after 28 days curing, there was an improvement of mechanical properties due to the presence of the  
111 pyrolyzed nanoparticles. The better percentages of addition were the same as those of the 7 days  
112 mechanical tests [16].

113 8. Coarse particles of pyrolyzed hazelnut shells, already investigated at nanoscale, were used to evaluate  
114 the mechanical properties of cement-based composites. The particle size distribution used was in the  
115 range of a few microns up to 140  $\mu\text{m}$ . Experimental results demonstrated that it was possible to use  
116 pyrolyzed materials with coarser particle size, ensuring the improvement of mechanical properties in  
117 terms of flexural and compressive strength, but not in terms of ductility, which was observed only  
118 when using smaller particles. In this case, the lowest percentage of addition (0.5 wt%) was optimal,  
119 showing an increment of 48% and of 62% at 7 days and of 23% and 61% at 28 days for flexural and  
120 compressive strength, respectively. Presumably, since the carbonaceous particles are coarser, a small  
121 percentage of them is enough to fill only the larger pores in the matrix, providing enhanced mechanical  
122 properties to the cementitious composites. Results showed an increase of fracture energy at 7 days  
123 with the maximum measured value for 0.8 wt% of biochar content (84% greater fracture energy with  
124 respect to the plain specimens). On the other hand, at 28 days, this increment vanished, and a decrease  
125 of fracture energy was observed for all mixtures (with decrements between 17% for 0.5 wt% of  
126 particles addition and of 4% for the addition of 1 wt%) [17].

127 Although these results were satisfactory in terms of mechanical properties, self-produced biochar cannot be

128 considered at zero cost, as the annealing and functional procedures and energy consumption for grinding  
 129 procedures both impact on the sustainability of the material. Furthermore, research has so far to address the  
 130 reproducibility of cement mixtures. For this reason, the present work investigates the effectiveness of the  
 131 standardized biochar, Softwood Biochar SWC, with the main goal of ensuring the reproducibility of  
 132 cementitious mixtures. The material used is a biochar provided by the UK Biochar Centre produced from  
 133 pyrolyzed feedstock with a nominal peak temperature of 700°C, which has a carbon content of 90.21 wt% and  
 134 a stability of 97.27 % C-basis. The investigated additions were 0.8 wt% and 1 wt% according to the cement  
 135 weight [18]. Experimental results obtained by three point bending tests showed that the standardized biochar  
 136 generally improves mechanical properties of cement-based composites.

137

138

## 139 2. Materials and methods

### 140 2.1 Manufacturing of materials and specimens

141 Ordinary Portland Cement, OPC, deionized water, superplasticizer and biochar were used to prepare cement  
 142 mixtures. OPC (CEM I 52.5 R) was produced by Ciments Vigier SA. It is characterized by the rapid  
 143 development of the initial resistance, in accordance to the harmonized European standard UNI EN 197/1 and  
 144 is labeled with CE marking according to European Regulation 305/2011 (CPR). Its composition, physical,  
 145 mechanical, and chemical requirements are reported in Tables 1-3.

146

147

Table 1. Cement – Composition.

Type	Designation	Notation	Clinker Portland	Secondary Constituents
CEM I	Cement Portland	CEM I	95-100%	0-5%

148

149

Table 2. Cement – Physical and Mechanical Requirements.

Class of Strength	Setting time (min)	Stability (mm)
52.5 R	$\geq 45$	$\leq 10$

Table 3. Cement - Chemical Requirements.

Properties	Requirements	Indicative Values Vigier
Sulphate Content	$\leq 4.0 \%$	$<3\%$
Chloride Content	$\leq 0.10 \%$	$<0.06\%$

150

151

152 Superplasticizer (Isoflow6600), produced by Cemex, was used to achieve a good workability of the mix and,  
 153 in the meanwhile, to reduce the w/c ratio to 0.35; its additional percentage according to the weight of cement  
 154 was 1 wt%. Its characteristics are shown in Table 4.

155

Table 4. Characteristics of Superplasticizer “Isoflow6600” of Cemex.

Characteristics	Value	Regulation
Form	liquid	
Color	light brown	
pH (at 20 °C)	$6.1 \pm 1$	ISO 4316
Boiling Temperature	100 °C	
Density (at 20 °C)	$1.08 \pm 0.02 \text{ g/cm}^3$	ISO 758
Solubility	soluble in water	

156

157 Softwood Biochar SWC was added as nano/microparticles in the cementitious composites. The investigated  
 158 additions were 0.8 wt% and 1 wt% according to the cement weight in line with previous studies [17]. Its basic  
 159 utility properties, the production parameters and the toxicant reporting are shown in the Tables 5-7.

160

Table 5. SWC Basic Utility Properties.

Properties	Unit of measure	Value
Moisture	wt %	1.00
C <sub>tot</sub>	wt %	90.21
H	wt %	1.83
O	wt %	6.02
C <sub>org</sub>	wt %	tbd*
H:C <sub>org</sub>	Molar ratio	tbd*
H:C <sub>tot</sub>	Molar ratio	0.24
O:C <sub>tot</sub>	Molar ratio	0.05
Total ash	wt %	1.89
Total N	wt %	$< 0.01$
pH	-	8.44
Electric conductivity	dS/m	0.16
Biochar C stability	% C-basis	97.27

161

\*tbd = to be defined in next version,

162

163

Table 6. SWC Toxicant Reporting - Total Content

Toxicity	Unit of measure	Value
Dioxin/ Furan (PCDD/ Fs)	mg/kg dry wet	3.30
Polycyclic Aromatic Hydrocarbons (EPA16)	mg/kg dry wet	0.18
Polychlorinated Biphenyls (PCBs)	mg/kg dry wet	0.17
As	mg/kg dry wet	0.61
Cd	mg/kg dry wet	8.16
Cr	mg/kg dry wet	123.35
Co	mg/kg dry wet	4.37
Cu	mg/kg dry wet	9.66
Pb	mg/kg dry wet	bdl*
Hg	mg/kg dry wet	bdl*
Mo	% C-basis	38.54
Ni	mg/kg dry wet	74.07
Se	mg/kg dry wet	bdl*
Zn	mg/kg dry wet	99.60

164

\* bdl = below detection limit

165

166

Table 7. SWC Production Parameters

Parameters	Unit of measure	Value
Nominal HTT*	°C	700
Max. char HTT*	°C	680
Reactor wall temp.	°C	700
Heating rate	°C	680
Kiln residence time	min	12
Mean time at HTT*	min	5
Biochar yield	wt %	87
Pyrolysis liquid yield	wt %	27.64
Pyrolysis gas yield	wt %	54.05
Pyrolysis liquid HHV*	MJ/kg	1.06
Pyrolysis gas HHV*	MJ/kg	12.6

167

\*HTT=highest treatment temperature, HHV = higher heating value

168 The standardized biochar SWC was first manually ground in agate mortar with an agate pestle and then sieved

169 with a 125 µm sieve. Subsequently, it was milled in ethanol in agate jars with agate balls (5 mm in diameter)

170 in a planetary mill (Pulverisette 5) (Figure 1).

171



172 Fig. 1: SWC Biochar - Grinding operation with planetary multi-station mill

173 At the end of each grinding cycle the particle sizes were measured by means of laser granulometry “Analysette  
174 22 Compact” of Fritsch. (Figure 2) Biochar-ethanol solution was finally placed into the oven for a few days in  
175 order to dry the material and then it was pulverized to make it ready for cement mixes preparation.

176



177 Fig. 2: SWC Biochar - Granulometric Analysis.  
178

179

180 For each experimental set (OPC - Sp 1%; SWC 0.8% - Sp 1%; SWC 1% - Sp 1%), 8 specimens were prepared,  
181 (two steel formworks, made up of four 20 x 20 x 80 mm<sup>3</sup> prismatic moulds) 4 of whom were tested after 7  
182 days of curing and the remaining 4 were tested after 28 days of curing (Table 8).

Table 8. Set of Experimental Specimens

Mixture ID	Number specimens (7 days of curing)	Number specimens (28 days of curing)
OPC - Sp 1%	4	4
SWC 0.8% - Sp 1%	4	4
SWC 1% - Sp 1%	4	4

185

186 Table 9 shows the mix-design used to prepare the three sets of the experimental specimens. The water/cement  
 187 ratio was fixed to 0.35 and the additional percentage of the superplasticizer with respect to the weight of cement  
 188 was 1%, while the pyrolyzed nanoparticles were added in different percentages (0.8 wt% and 1 wt%) with  
 189 respect to the weight of cement.

190

191

Table 9. Cement mix-design

Materials		Mix-design N° 1	Mix-design N° 2	Mix-design N° 3
		0%* SWC	0.8%* SWC	1%* SWC
Cement	[g]	230	230	230
Water	[g]	80.5	80.5	80.5
w/c ratio	[-]	0.35	0.35	0.35
Superplasticizer	[g]	2.3	2.3	2.3
Biochar SWC	[g]	0	1.84	2.3

\*with respect to the weight of cement

192

193

194 All the materials were first weighed according to the amounts reported in table 9. Deionized water,  
 195 superplasticizer and the standardized biochar were weighed and mixed together inside a plastic beaker,  
 196 subsequently immersed in an ultrasonic bath for 10 minutes in order to allow a good mixing and  
 197 homogenization suspension. Then, the cement was gradually added into the suspension within the first minute  
 198 and the mixture was subjected to mechanical mixing by means of a vertical rod agitator with a four wings steel  
 199 propeller with a direct motor with variation of speed, by taking care that the mixture remained fluid and  
 200 homogeneous. Specifically, in the first and in the second minute, the mixing was performed with the same  
 201 speed, while in the third and fourth mixing minutes the mixing speed was slightly increased. At the end of the

202 mixing phase, the cement mixture was slowly transferred into the steel formworks, made up of four 20 x 20 x  
203 80 mm<sup>3</sup> prismatic moulds, avoiding air entrainment. Then, the experimental specimens were stored inside these  
204 moulds in a humid atmosphere for at least 24 hours and, once they were demolded, they were immersed in  
205 water for 7 and 28 days curing.

## 206 2.2 Experimental tests

207 Through the Scanning Electron Microscope with Field Emission source (FE-SEM, Zeiss Merlin) it was  
208 possible to characterize the morphology of the particles with a resolution around the nanometer.

209 Each experimental specimen was submitted to Three Point Bending test. Before performing the TPB tests, a 6  
210 mm in depth and 2 mm in width notch was realized on each specimen by means of a metallographic truncator  
211 “TR 100 S Remet” in the centre line of the specimen on the face orthogonal to the casting surface, according  
212 to JCI-S-001 recommendation [19]. The TPB tests were performed using a Zwick Line-Z050, a single column  
213 displacement-controlled testing machine with a load cell of 1 kN. All the specimens were tested in Crack  
214 Mouth Opening Displacement mode (CMOD) through a clip-on gauge (Figure 3). A span of 65 mm and a test  
215 speed of 0.005 mm/min were adopted.

216 Flexural strength,  $\sigma_f$ , was determined as it follows [19]:

217

$$218 \quad \sigma_{f,max} = F_{max} \cdot \frac{3L}{2bh^2} \quad [MPa] \quad (1)$$

219

220 in which  $L$  is the span equal to 65 mm,  $b$  is the specimen depth equal to 20 mm and  $h$  is the net ligament height  
221 equal to 14 mm.

222 The TPB tests let to evaluate Fracture Energy,  $G_F$ , by using the equation proposed in the JCI-S-001 standard  
223 [19]:

224

$$225 \quad G_F = \frac{0.75W_0 + W_1}{A_{lig}} = G_{F0} + G_{Fcorr} \quad \left[ \frac{N}{mm} \right] \quad (2)$$

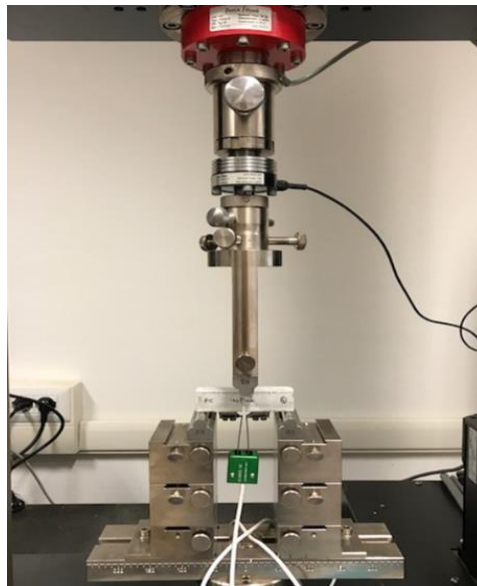
226

227 in which  $A_{lig}$  [mm<sup>2</sup>] is the area of the nominal ligament,  $W_0$  [N·mm] is the area below CMOD curve up to

228 rupture of specimen and  $W_l$  [N·mm] is the work done by deadweight of specimen and loading and defined as  
229 follow:

230 
$$W_1 = 0.75 \left( \frac{S}{L} m_1 + 2m_2 \right) g \cdot CMOD_c \quad [N \cdot mm] \quad (3)$$

231  
232 in which  $S$  is the loading span,  $L$  is the total length of specimen,  $m_1$  is the mass of the notched specimen,  $m_2$  is  
233 the mass of the loading arrangement part not attached to testing machine but placed on beam until rupture,  $g$   
234 is the gravity acceleration and  $CMOD_c$  is the crack mouth opening displacement at the rupture.



235  
236 Figure 3: Three Point Bending Test in CMOD control mode

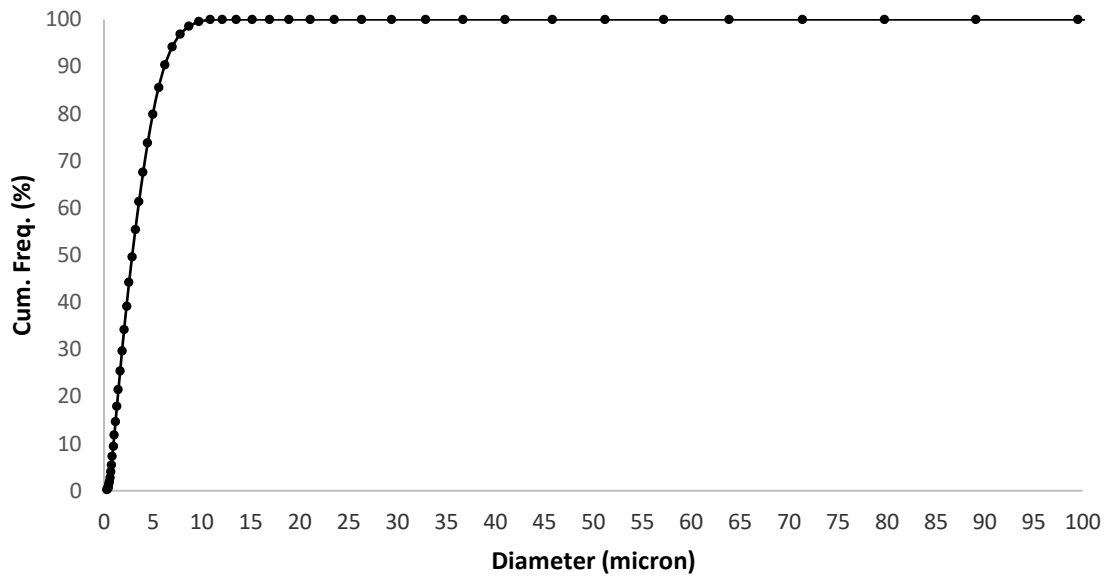
237

### 238 3. Results and discussion

#### 239 3.1 Biochar investigation

240 The average particle size reached was in the range between 2-6  $\mu\text{m}$ . (Figure 4).

241



242

243

Fig. 4: SWC Biochar - Granulometric Curve

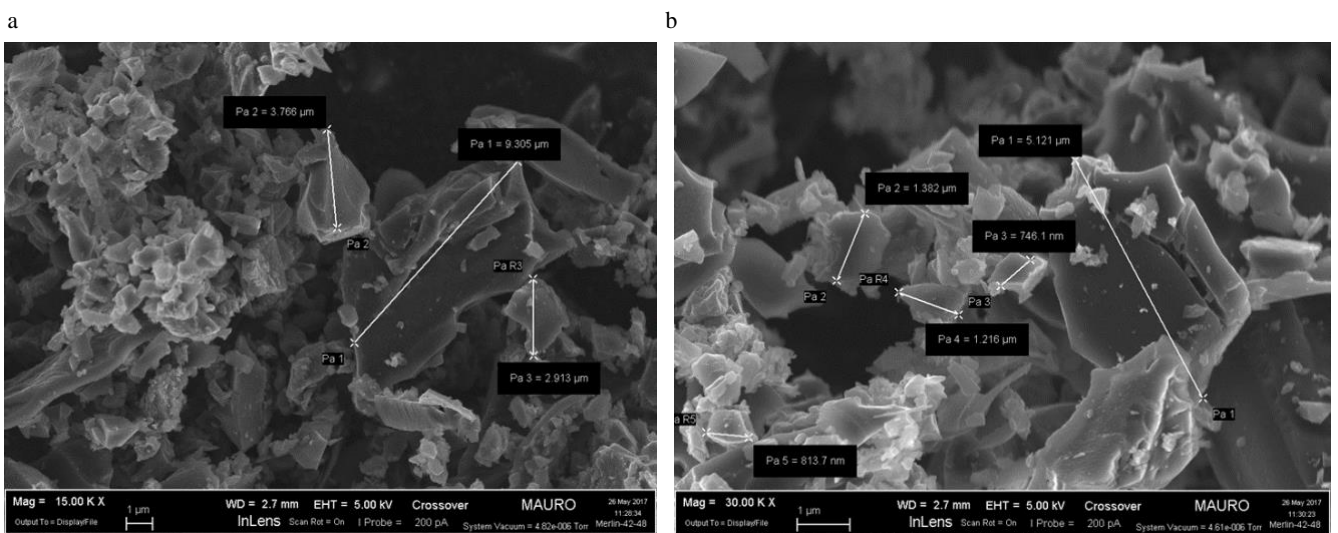
244

245 The images of FE-SEM measurements are reported in Figure 5 and confirmed laser granulometry results.

246 Particles have sharp edges, as expected from a ground brittle material.

247

248



249

250

Fig. 5: FE-SEM micrograph (a) 15 kx magnification; (b) 30 kx magnification

251

252 3.2 Composites mechanical testing

253 Experimental results obtained by TPB tests showed very interesting indications. In general, the standardized  
 254 biochar improved mechanical properties of cement-based composites compared to the standard ones. Results  
 255 reported in Table 10 (7 days tested specimens) and Table 11 (28 days tested specimens) were processed with  
 256 statistical tools, specifically the mean value and the standard deviation of the Maximum Force  $F_{max}$ , the  
 257 Flexural Strength  $\sigma_f$  and the Fracture Energy  $G_F$  were calculated:

258 Table 10. Experimental Results – TPB tests 7 days

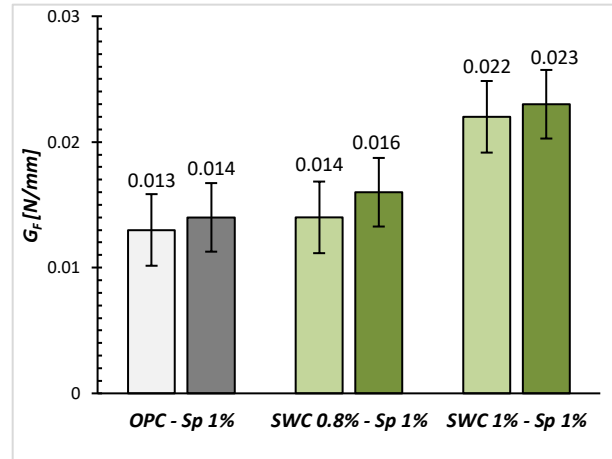
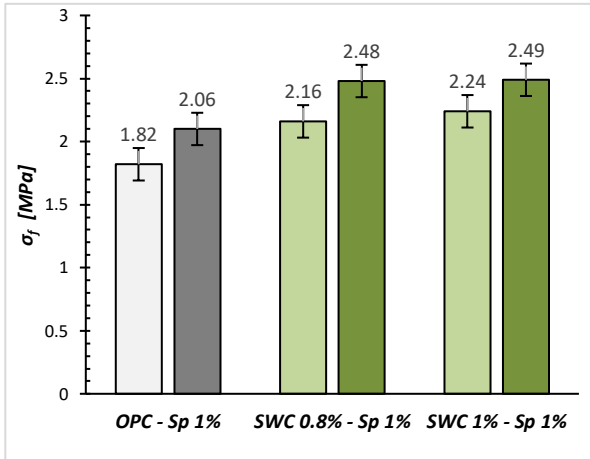
Specimen ID	N°	$F_{max}$ [N]	$F_{max}$ mean	$F_{max}$ st. dev.	$\sigma_f$ [MPa]	$\sigma_f$ mean	$\sigma_f$ st. dev	$G_F$ [N/mm]	$G_F$ mean	$G_F$ st. dev
OPC - Sp 1%	1	68.10			1.69			0.008		
OPC - Sp 1%	2	73.80	73.20	6.66	1.84	1.82	0.17	0.011	0.013	0.004
OPC - Sp 1%	3	82.40			2.05			0.018		
OPC - Sp 1%	4	68.50			1.70			0.014		
SWC 0.8 % - Sp 1%	1	75.20			1.87			0.010		
SWC 0.8 % - Sp 1%	2	78.40	83.88	8.72	1.95	2.16	0.23	0.010	0.014	0.004
SWC 0.8 % - Sp 1%	3	95.80			2.38			0.019		
SWC 0.8 % - Sp 1%	4	86.10			2.14			0.014		
SWC 1 % - Sp 1%	1	111.00			2.76			0.024		
SWC 1 % - Sp 1%	2	88.60	89.88	15.87	2.20	2.24	0.39	0.026	0.022	0.004
SWC 1 % - Sp 1%	3	87.40			2.17			0.017		
SWC 1 % - Sp 1%	4	72.50			1.80			0.022		

259  
 260 Table 11. Experimental Results – TPB tests 28 days

Specimen ID	N°	$F_{max}$ [N]	$F_{max}$ mean	$F_{max}$ st. dev.	$\sigma_f$ [MPa]	$\sigma_f$ mean	$\sigma_f$ st. dev	$G_F$ [N/mm]	$G_F$ mean	$G_F$ st. dev
OPC - Sp 1%	1	89.00			2.21			0.008		
OPC - Sp 1%	2	78.30	82.85	6.30	1.95	2.06	0.17	0.007	0.014	0.007
OPC - Sp 1%	3	76.60			1.91			0.020		
OPC - Sp 1%	4	87.50			2.18			0.020		
SWC 0.8 % - Sp 1%	1	101.00			2.51			0.009		
SWC 0.8 % - Sp 1%	2	78.60	99.71	15.82	1.95	2.48	0.48	0.012	0.016	0.007
SWC 0.8 % - Sp 1%	3	116.94			2.91			0.024		
SWC 0.8 % - Sp 1%	4	102.30			2.54			0.020		
SWC 1 % - Sp 1%	1	113.00			2.81			0.018		
SWC 1 % - Sp 1%	2	87.10	100.23	10.70	2.17	2.49	0.27	0.026	0.023	0.007
SWC 1 % - Sp 1%	3	98.44			2.45			0.030		
SWC 1 % - Sp 1%	4	102.37			2.55			0.016		

261  
 262 The specimens containing biochar showed a certain dispersion of the MOR values (Table 11). This was  
 263 probably due to the problems encountered during the preparation phase of the composites, such as the non-  
 264 uniform dispersion of the nanoparticles into the cement paste [20].  
 265 However, samples characterized by the addition of biochar have a greater flexural strength compared to the  
 266 plain cement, either at 7 days or at 28 days; this increase amounts to around 20%. Furthermore, there was no

267 substantial difference between the two biochar contents used (Figure 6). Starting from TPB tests, it was  
 268 possible to determine the Fracture Energy of the experimental specimens and it was observed that its mean  
 269 value slightly increased with the introduction of biochar in the cement, both after 7 and 28 days of curing  
 270 (Figure 7).



271

Fig. 6: TPB Test: Flexural strength – 7 and 28 days

Fig. 7: Fracture Energy – 7 and 28 days - JCI-S-001 standard

272  
 273  
 274

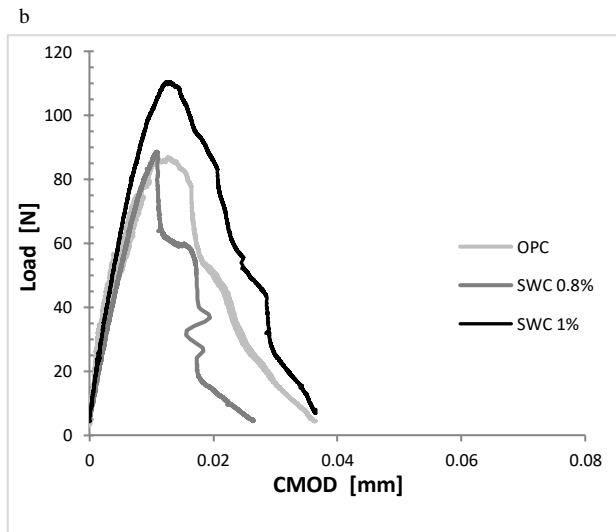
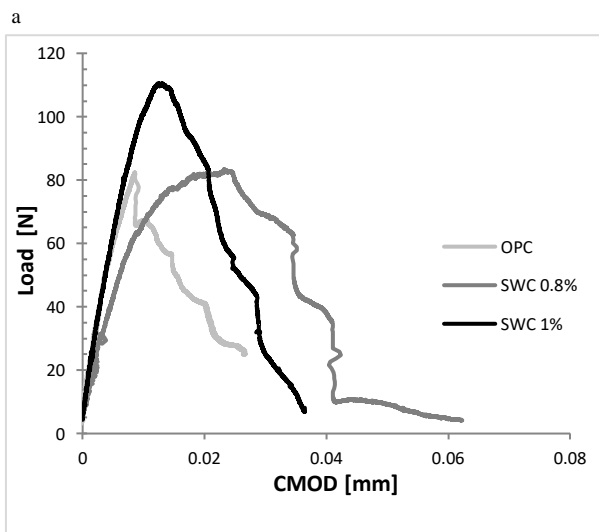


Fig. 8: (a) Load vs CMOD Curve, 7 days and (b) Load vs CMOD Curve, 28 days for the most significant tests

275  
 276  
 277

278 From the Load-CMOD curves graph (Figure 8) it was possible to notice that the pyrolyzed nanoparticles within  
 279 the cement-based composites led to a better mechanical behavior in terms of peak-load and post-peak response,  
 280 directly linked to the flexural strength and toughness results.

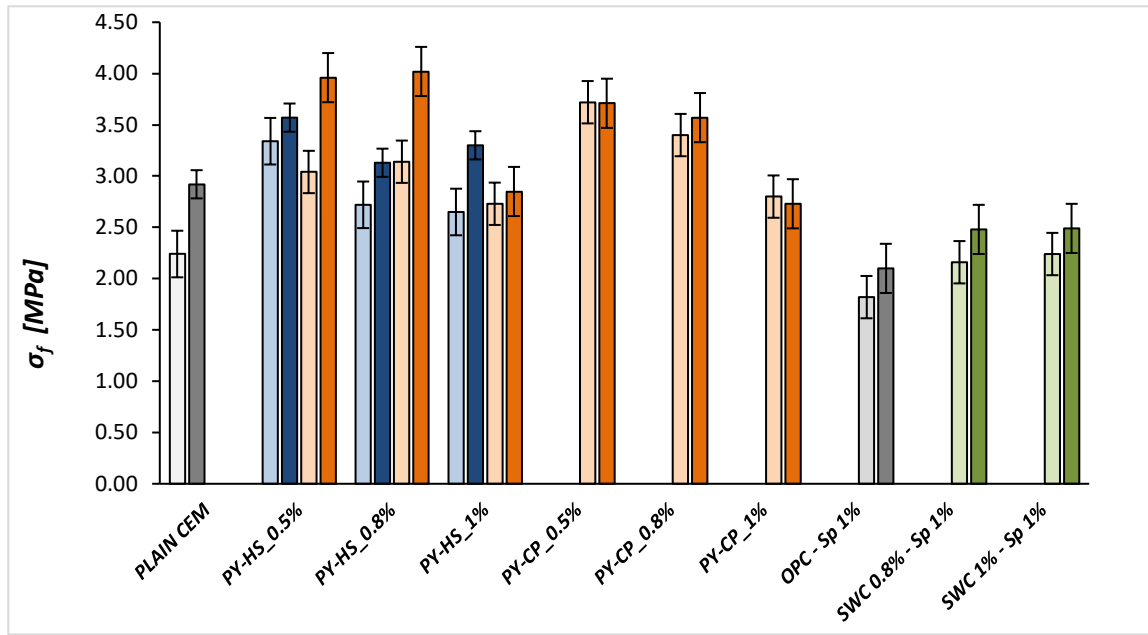
281 From the FE-SEM observations, the biochar particles showed sharp edges, irregular shapes and appeared very  
 282 porous. The carbon nanoparticles have a high surface-area to volume ratio (SA/V), that means an increment

283 of the contact area between the particles and the surrounding cementitious matrix, hence allowing a higher  
284 interaction with the matrix and more efficient behavior. This could lead to a good adhesion of the particles to  
285 the cement matrix. Moreover, the FESEM observations conducted in previous studies [16] showed that  
286 specimens with pyrolyzed material have a more tortuous fracture path and therefore less linear than the typical  
287 brittle fracture observed in cements. This could explain the variation in the post-peak behavior of the material  
288 and the increase in the ability to absorb energy before breaking [20].

### 289 *3.2 Comparison between past investigations and current research*

290 Previous studies on the effectiveness of biochar into cement-based materials demonstrated that it was possible  
291 to use pyrolyzed materials with coarser particle size, ensuring the improvement of mechanical properties in  
292 terms of flexural and compressive strength, but not in terms of toughness, obtained only when using smaller  
293 particles [17]. Restuccia and Ferro [17] used two different biomasses of agro-food wastes: coffee powder and  
294 hazelnut shells. For both types of biochar, the addition with respect to weight of cement was 0.5, 0.8 and 1 %.  
295 These materials were subjected to the pyrolysis process with a heating ramp of 6 °C/min and a final temperature  
296 set point of 800 °C. Analysis of Flexural Strength and Fracture Energy results demonstrated that the most  
297 effective additional percentage for pyrolyzed hazelnut shells was 0.8 wt%, while for coffee powder it was 0.5  
298 wt%. In the present work, it was possible to notice that  $\sigma_f$  and  $G_F$  increased with the increasing content of  
299 biochar. Nonetheless, the average values of  $F_{max}$ ,  $\sigma_f$  and  $G_F$  in the present work were generally lower than those  
300 reported in [20] although using pyrolyzed materials with comparable sizes (Figures 9-10).

301



302

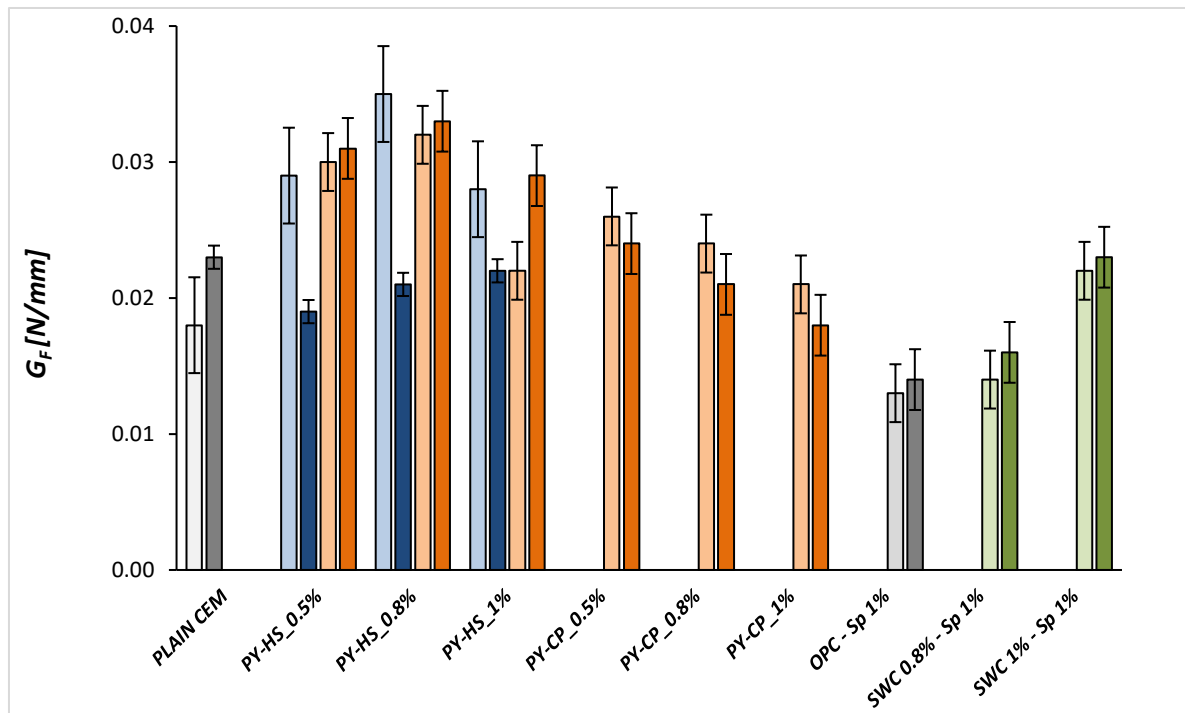
303

304

305

306

Fig. 9: Flexural Strength - Comparison between PY-HS (micro and nano), PY-CP [17] and SWC [18] specimens, 7 and 28 days. (PY-HS=pyrolyzed hazelnut shell, PY-CP=pyrolyzed coffee powder, SWC= Softwood Char)



307

308

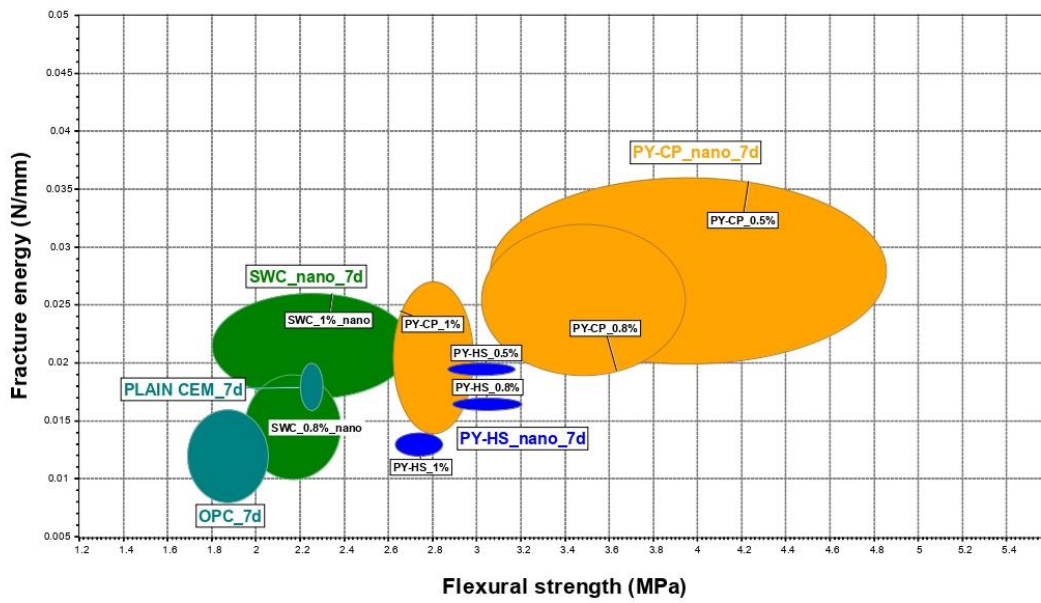
309

310

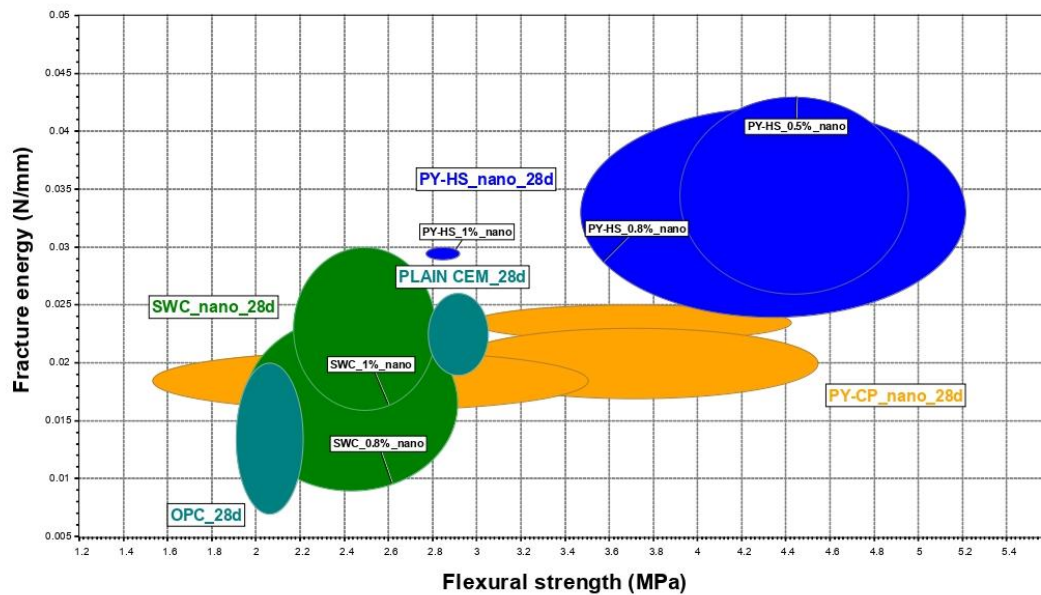
311

Fig.10: Fracture Energy - Comparison between PY-HS (micro and nano), PY-CP [17] and SWC [18] specimens, 7 and 28 days (PY-HS=pyrolyzed hazelnut shell, PY-CP=pyrolyzed coffee powder, SWC= Softwood Char)

312 The Figures 11-12 show the flexural strength vs fracture energy, in a linear scale, after 7 and 28 days of  
 313 curing. The material charts map the areas of property space occupied by each material class. Materials families  
 314 (standard cement and cement with nanoparticles of SWC, PY-HS, PY-CP) are identified by colors. In the  
 315 graph, the experimental specimens characterized by the addition of carbon nanoparticles are placed in the  
 316 upper right position with respect to the specimens without the addition of biochar, that means better  
 317 performance as they have higher flexural strength and fracture energy.



318  
 319 Fig.11: Ashby map of Flexural Strength vs Fracture Energy - 7 days [25]. The colors represents families of materials.



320  
 321 Fig.12: Ashby map of Flexural Strength vs Fracture Energy - 28 days [25]. The colors represents families of materials.

322 The percentage of carbon inside the standardized biochar, SWC, used in this work (90.21%) is lower than the  
323 one of self-produced biochar used in the previous study [20] (97.8%) as well as the pyrolysis temperature  
324 (700°C compared to 800°C). These two features have a great influence on the yield and efficiency of biochar  
325 production, as also highlighted by other literature studies [21-22]. Gupta and Kua [21] underlined biochar key  
326 production factors (specifically, pyrolysis temperature, heating rate, pressure) that determine the potential of  
327 biochar as a carbon capturing and sequestering construction material.

328 Other results were analyzed to understand the effectiveness of biochar and the influence of the pyrolysis  
329 conditions on mechanical properties of cementitious composites. Montenegro et al [23] found that strength and  
330 ductility increased by adding a percentage equal to 0.08 wt% of pyrolyzed coffee particles into the cementitious  
331 matrix. In fact, the  $F_{MAX}$  grew from 130 N to about 180 N and, at the same time, fracture energy increased by  
332 40%. The pyrolysis of coffee powder, cocoa husk and parchment coffee, rice husk and hazelnut shell pellets  
333 was carried out. The influence of two different conditions on the mass and energy distribution of the products  
334 obtained was studied. The hazelnut shell biomass substrate generated the highest energetic chemical energy  
335 yield (86%). These inert carbonized particles can generate high performance cement composites, by increasing  
336 the compressive strength, the peak load under bending, and their fracture energy and can improve the post  
337 peak response. These inert carbonized particles also modify the fracture path, thus resulting in a larger fracture  
338 zone.

339 These results agree with [24], where air-dried spruce wood was pyrolyzed up to 2400°C. These authors  
340 determined by means of the nanoindentation technique that mechanical properties of heat treated materials  
341 could roughly be divided into three temperature regions: (i)  $T < 400^{\circ}\text{C}$ , (ii)  $400 < T < 1000^{\circ}\text{C}$  and (iii)  $T > 1000^{\circ}\text{C}$ .  
342 Specifically, in the temperature range from 600° to 1000°C, the elastic modulus linearly increased from about  
343 20 to 40 GPa. At around 800°C, the elastic modulus and the hardness reached their maximum values. The rise  
344 of the Young's modulus and hardness can be correlated to the increase in the density of the material observed  
345 between 600° and 900°C as well as to the increasing formation of covalent carbon bonds.

346

#### 347 **4. Conclusions**

348 Nowadays, pressing environmental issues mean that it is imperative for new building materials to perform  
349 better and have a manufacturing process which is energy-efficient and sustainable.

350 In line with previous experimental studies, present research focused on the use of standardized biochar in  
351 cement-based composites in different percentages of addition with respect to the weight of cement. In previous  
352 studies [17-20], biochar used was self-produced through the pyrolysis of agro-food waste unlike that used in  
353 the present work which was standardized in view of a possible industrial production of biochar cement-based  
354 composites. Results of the mechanical tests showed a promising improvement in strength and toughness. In

355 fact, higher flexural strength and fracture energy values were recorded for specimens with the addition of  
356 biochar compared to those of the plain cement specimens.  
357 However, the flexural strength and fracture energy results were lower than those of previous studies [17-20].  
358 This could be linked to the different pyrolysis parameters used in the production of biochar such as temperature,  
359 heating rate or pressure. Results could therefore be influenced by the type of carbonaceous material and by the  
360 production parameters (which influence the formation of strong covalent carbon bonds) rather than by the  
361 carbon particles size. Selection of suitable conditions to produce a biochar with desired properties therefore  
362 requires knowledge of dependencies and influencing factors. From an economic point of view, these carbon  
363 particles are low-cost, as they are a by-product of the biomass pyrolysis process. For this reason, they are a  
364 valid material for new green construction materials.

365  
366  
367  
368

## REFERENCES

- 369 [1] M. S. Imbabi, C. Carrigan, S. McKenna “Trends and developments in green cement and concrete  
370 technology”, *International Journal of Sustainable Built Environment* (2012) 1, 194–216
- 371 [2] K. Weber, P. Quicker “Properties of biochar” *Review article Fuel* 2017 (2018) 240-261
- 372 [3] A. Mohd, W. A. W. A. K. Ghani, N. Z. Resitanim and L. Sanyang, "A Review: Carbon Dioxide Capture:  
373 Biomass- Derived-Biochar and Its Applications," *Journal of Dispersion Science and Technology*, vol. 34:7,  
374 pp. 974-984, 2013.
- 375 [4] M. Bardalai and D. K. Mahanta, "Characterization of Biochar Produced by Pyrolysis from Areca Catechu  
376 Dust," *Materials Today: Proceedings*, vol. 5, pp. 2089-2097, 2018.
- 377 [5] Schmidt, H.P., “55 Uses of Biochar”, *Ithaca Journal*, 1, pp. 286–289, 2012
- 378 [6] D. Ziegler, P. Palmero, M. Giorelli, A. Tagliaferro, J.M. Tulliani, “Biochars as innovative humidity  
379 sensing materials”, *Chemosensors*, vol. 5, 4 (2017): 35.
- 380 [7] P. Jagdale, D. Ziegler, M. Rovere, J.M. Tulliani, A. Tagliaferro, “Waste coffee ground biochar: A material  
381 for humidity sensors”, *Sensors*, vol. 19, 4 (2019): 801.
- 382 [8] R.A. Khushnood, S. Ahmad, L. Restuccia, C. Spoto, P. Jagdale, J.M. Tulliani, G.A. Ferro, “Carbonized  
383 nano/microparticles for enhanced mechanical properties and electromagnetic interference shielding of  
384 cementitious materials”, *Frontiers of Structural and Civil Engineering*, Vol. 10 (2016) 209-213.
- 385 [9] Schmidt, H.P., “Biochar as building material for an optimal indoor climate” *Freitag*, 4, 2014.
- 386 [10] G.A. Ferro, S. Ahmad, R.A. Khushnood, L. Restuccia, J.M. Tulliani, “Improvements in self-consolidating  
387 cementitious composites by using micro carbonized aggregates”, *Frattura ed Integrità Strutturale*, Vol. 30  
388 (2014) 75-83.
- 389 [11] ASTM C1018-97 “Standard test method for flexural toughness and first-crack strength of fiber reinforced  
390 concrete (using beam with third-point loading)” (1997) 7.

- 391 [12] G.A. Ferro, J.M. Tulliani, P. Jagdale, L. Restuccia, “New Concepts for Next Generation of High  
392 Performance Concretes”, *Procedia Materials Science*, Vol. 3 (2014), 1760-1766.
- 393 [13] R.A. Khushnood, S. Ahmad, G.A. Ferro, J.M. Tulliani, L. Restuccia, P. Jagdale, “Modified fracture  
394 properties of cement composites with nano/micro carbonized bagasse fibers” *Frattura ed Integrità Strutturale*,  
395 Vol. 34 (2015) 534- 542.
- 396 [14] S. Ahmad, J.M. Tulliani, G.A. Ferro, R.A. Khushnood, L. Restuccia, P. Jagdale “Crack path & fracture  
397 surface modifications in enhanced cement composites” *Frattura ed Integrità Strutturale*, Vol. 34 (2015) 524-  
398 533.
- 399 [15] L. Restuccia, G.A. Ferro, “Nanoparticles From Food Waste: A “Green” Future For Traditional Building  
400 Materials”, 9th International Conference on Fracture Mechanics of Concrete and Concrete Structures  
401 FraMCoS-9, 2016.
- 402 [16] L. Restuccia, G.A. Ferro “Promising low cost carbon-based materials to improve strength and toughness  
403 in cement composites” *Construction and Building Materials* 126 (2016) 1034–1043.
- 404 [17] L. Restuccia, G.A. Ferro “Influence of filler size on the mechanical properties of cement-base  
405 composites”, *Fatigue and Fracture of Engineering Materials and Structures* 41(2018) 797-805.
- 406 [18] I. Cosentino “The use of Bio-char for sustainable and durable concrete”, Master thesis, Politecnico di  
407 Torino, 2017.
- 408 [19] JCI-S-001, Method of Test for Fracture Energy of Concrete by use of Notched Beam, Japan Concrete  
409 Institute, 2003.
- 410 [20] L. Restuccia “Re-think, Re-use: agro-food and C&D waste for high-performance sustainable cementitious  
411 composites”, Ph.D. Thesis, Politecnico di Torino, 2016.
- 412 [21] S. Gupta and H. W. Kua “Factors Determining the Potential of Biochar as a Carbon Capturing and  
413 Sequestering Construction Material\_ Critical Review “, *Journal of Materials in Civil Engineering*, 29 (9)  
414 (2017).
- 415 [22] S. Gupta, H. W. Kua, Sin Yee Tan Cynthia “Use of biochar-coated polypropylene fibers for carbon  
416 sequestration and physical improvement of mortar”, *Cement and Concrete Composites* 83 (2017) 171-187.
- 417 [23] Y.S. Montenegro Camacho, S. Bensaid, B. Ruggeri, L. Restuccia, G.A. Ferro, G. Mancini, D. Fino,  
418 “Valorisation of by-Products/Waste of Agro-Food Industry by the Pyrolysis Process”, *Journal of Advanced*  
419 *Catalysis Science and Technology*, Vol. 3 (2016) 1-11.
- 420 [24] G. A. Zickler, T. Schöberl, O. Paris, “Mechanical properties of pyrolyzed wood: a nanoindentation study”,  
421 *Philosophical Magazine*, vol. 86, 10 (2006) 1373–1386.
- 422 [25] CES EduPack Software, 2018, Granta Design.

423

424

425